Modelling of blended Diesel and biodiesel fuel droplet heating and evaporation

Al Qubeissi, M, Sazhin, SS & Elwardany, AE

Original citation & hyperlink:
Al Qubeissi, M, Sazhin, SS & Elwardany, AE 2017, 'Modelling of blended Diesel and biodiesel fuel droplet heating and evaporation' *Fuel*, vol 187, pp. 349-355
http://dx.doi.org/10.1016/j.fuel.2016.09.060

DOI 10.1016/j.fuel.2016.09.060
ISSN 0016-2361
ESSN 1873-7153

Publisher: Elsevier

Modelling of blended Diesel and biodiesel fuel droplet heating and evaporation

M. Al Qubeissi[a*], S.S. Sazhin[b], A.E. Elwardany[c]

[a]*Centre for Mobility & Transport, School of Mechanical, Aerospace and Automotive Engineering, Coventry University, Coventry CV1 2JH, United Kingdom*

[b]*Sir Harry Ricardo Laboratories, Advanced Engineering Centre, School of Computing, Engineering and Mathematics, University of Brighton, Brighton BN2 4GJ, United Kingdom*

[c]*Mechanical Engineering Department, Faculty of Engineering, Alexandria University, Alexandria 21544, Egypt*

Abstract

The paper presents a new approach to the modelling of heating and evaporation of dual-fuel droplets with a specific application to blends of biodiesel (represented by the widely used soybean methyl ester, SME) and Diesel fuels in conditions representative of internal combustion engines. The original compositions, with up to 105 components of Diesel and biodiesel fuels, are replaced with a smaller number of components and quasi-components using the recently introduced multi-dimensional quasi-discrete (MDQD) model. Transient diffusion of these components and quasi-components in the liquid phase and temperature gradient and recirculation inside droplets are taken into account. The results are compared with the predictions of the case when blended biodiesel/Diesel fuel droplets are represented by pure biodiesel fuel or pure Diesel fuel droplets. It is shown that droplet evaporation time and surface temperature predicted for 100% SME, representing pure biodiesel fuel, are close to those predicted for pure Diesel fuel. Also, it is shown that the approximations of the actual compositions of B5 (5% SME and 95% Diesel) and B50 (50% SME and 50% Diesel) dual-fuels by 17 quasi-components/components, using the MDQD model, lead to under-predictions in droplet lifetimes by up to 9% and 4%, respectively, under the same engine conditions. The application of the latter model has resulted in above 83% reduction in CPU time compared to the case when all 105 components are taken into account using the discrete component model.

Keywords: Biodiesel fuel; Diesel fuel; Droplet heating; Fuel blends; Heating and evaporation; Multi-component droplets.

*Corresponding author, Email Mansour.alQubeissi@Coventry.ac.uk, Tel. +44 (0)2477 465 8060

1. Introduction

The interest in Diesel and biodiesel fuel blends has been mainly stimulated by depletion of fossil fuels and the need to reduce carbon dioxide emissions that contribute towards climate change [1,2]. The use of biodiesel

fuel is expected to contribute to the reduction of global warming [3]. Also, using a blend of biodiesel fuel as an alternative to pure fossil fuels has a number of other advantages: it is less polluting, cost effective, it has higher lubricity and a higher flash point, and it can be used in Diesel engines with minimal, or no, modifications [4–8]. According to the U.S. Environmental Protection Agency Tier I and Tier II standards (see [9] for details), fatty acid methyl ester (FAME) biodiesel types produced over the last decade pass the testing requirements for health effects [10].

Studies on the heating and evaporation processes of automotive fuel droplets are crucial to the design of internal combustion engines and to ensuring their good performance [11,12]. Accurate modelling is essential to the understanding of these processes and ultimately to the improvement of engine design. Previous studies of these processes have been either based on the analysis of individual components (Discrete Component (DC) model [13,14]), or on the probabilistic analysis of a large number of components (continuous thermodynamics [15–17] and the distillation curve [18–20] models). The first approach is generally applicable to cases when a relatively small number of components needs to be taken into account to avoid computationally expensive runs. In the second approach a number of simplifying assumptions are commonly used; for example, the species inside droplets are assumed to mix infinitely quickly (infinite diffusivity model).

The DC model based on the analytical solutions to the heat transfer and species diffusion equations was suggested in [21] and validated against experimental data in [22]. In our analysis, the predictions of the new simplified models will be compared with the prediction of the above-mentioned version of the DC model, taking into account the contributions of all components. Direct applications of this model were limited to the case when the number of components in fuels was relatively small (e.g. biodiesel fuels). In the case of fossil, or blended-fossil, fuels (containing potentially hundreds of components), however, the DC model would be computationally very expensive when directly applied to the modelling of droplet heating and evaporation. In response to this problem, the multi-dimensional quasi-discrete (MDQD) model was introduced in [23]. In this model, a large number of components was replaced with a much smaller number of components/quasi-components (C/QC) without losing the main features of the DC model. This model was applied to the analysis of heating and evaporation of realistic Diesel and gasoline fuel droplets [23,24]. It was shown to accurately predict the droplets' lifetimes and surface temperatures and to be computationally efficient [12].

In this paper, the analysis presented in [23,24] is generalised to the case of blended biodiesel/Diesel fuel droplets. The main features of the model used in our analysis and fuel compositions are summarised in Section 2. The results of calculations are presented in Section 3. The main results of the paper are summarised in Section 4.

2. Model and fuel compositions

As in [23,24], our analysis is based on the assumption that droplets are spherically symmetric. The MDQD model, in which the actual composition of fuel is reduced to a much smaller number of representative components/quasi-components (C/QC), is used.

The concept of quasi-components was first introduced in [25] and is based on a replacement of several actual alkane components with close carbon numbers n by a new alkane component with an average value of n, taking into account molar fractions of the original components. This averaging procedure led to non-integer values of n for the new component, in most cases, which do not have any physical meaning as components with non-integer values of n do not exist. Hence, we called these new components quasi-components. Although quasi-components are not real components, they were treated as real for the analysis of heat/mass transfer processes in droplets. In [23,24] the concept of quasi-components was generalised to include other groups of components (e.g. cycloalkanes, aromatics). Please note, however, that the selection of these C/QCs was based on trial and error. We are still working on the development of a more rigorous algorithm for this selection.

The effects of finite liquid thermal conductivity, diffusions of C/QCs in the liquid phase and recirculation inside droplets are taken into account using the Effective Thermal Conductivity/Effective Diffusivity (ETC/ED) models. The analysis is based on the previously obtained analytical solutions to the heat transfer and species diffusion equations within droplets (see [11]). The blended-fuel vapour is replaced with the vapour of n-dodecane; the binary diffusion coefficient of n-dodecane vapour in air is estimated as [26]:

$$D_{va} = 5.27 \times 10^{-6} \left({T_{\mathrm{ref}}}/{300}\right)^{1.583} p^{-1} \ (\mathrm{m^2\ s^{-1}}), \tag{1}$$

where $T_{\mathrm{ref}} = \frac{2}{3}T_s + \frac{1}{3}T_g$ is the reference temperature (in K), T_s and T_g are droplet surface and ambient gas temperatures, respectively, and p is ambient pressure (in bar).

The diffusion coefficient for liquid species is estimated using the Wilke-Chang approximation [23,27]:

$$D_l = \frac{7.4\times10^{-15} T\sqrt{\overline{M}}}{\mu_l {V_v}^{0.6}}, \tag{2}$$

where $\overline{M}$ is the average molar mass (in $\frac{\mathrm{kg}}{\mathrm{kmole}}$) of all components based on their mass fractions at the surface of the droplet, V_v is estimated as [23,27]:

$$V_v = \left({\sigma}/{1.18}\right)^3, \tag{3}$$

σ is the Lennard-Jones length (in Å), estimated as [27,28]:

$$\sigma = 1.468\overline{M}^{0.297}. \tag{4}$$

As in [23,24,29], all liquid properties are calculated at the average temperature inside droplets and all gas properties are calculated at the reference temperature T_{ref}; enthalpy of evaporation and saturated vapour pressure are estimated at the droplet surface temperature T_s.

The effects of thermal radiation are ignored in our analysis. These effects for heating and evaporation of mono-component droplets were studied in a number of papers including [26,30]. For sufficiently high radiative temperatures, it was shown that this effect leads to the non-monotonic approach of the surface temperature of a heated and evaporated droplet to the wet bulb temperature. We anticipate a similar effect during heating and evaporation of multi-component droplets, although this process has not been investigated to the best of our knowledge.

FAME biodiesel can be blended with Diesel fuel in various proportions. The most common blends are: B100 (pure biodiesel), B20 (20% biodiesel, 80% Diesel), B5 (5% biodiesel, 95% Diesel) and B2 (2% biodiesel, 98% Diesel) [8,31,32]. Note that B5 can be called Diesel fuel, with no separate labelling required at the pump [8], although no comparative analysis of heating and evaporation characteristics of droplets of these fuels, including droplet lifetimes, has been performed to the best of our knowledge.

The molar fractions of methyl esters in biodiesel fuel, assumed to be soybean methyl esters (SME), are inferred from the data reported in [29]; and those for Diesel fuel hydrocarbons are inferred from [23] (see Appendix A). Our analysis is focused on the following Diesel-biodiesel fuel blends: B80 (80% SME and 20% Diesel), B50 (50% SME and 50% Diesel), B20, and B5. The following cases will be considered: (1) pure SME (B100), taking into account the contributions of all 7 components, using the DC model; (2) the mixtures B5, B20, B50 and B80, taking into account all 105 components (7 components of SME and 98 components of Diesel fuel), using the DC model; (3) pure Diesel fuel, taking into account the contributions of 98 components (B0), using the DC model; and (4) the mixture B50, taking into account the contributions of all 105 components, using the MDQD model.

3. Results

The plots of droplet surface temperatures T_s and radii R_d versus time for biodiesel (SME) and Diesel fuels and their blends, taking into account the contributions of all 105 components, as predicted by the DC model, are shown in Fig. 1. As in [23], the initial droplet radius is taken equal to 12.66 μm, its axial velocity in still air (assumed constant) and initial temperature are assumed equal to U_{drop}= 10 m/s and T_d = 360 K, respectively; ambient air (gas) pressure and temperature are assumed equal to p_g = 32 bar and T_g = 700 K, respectively.

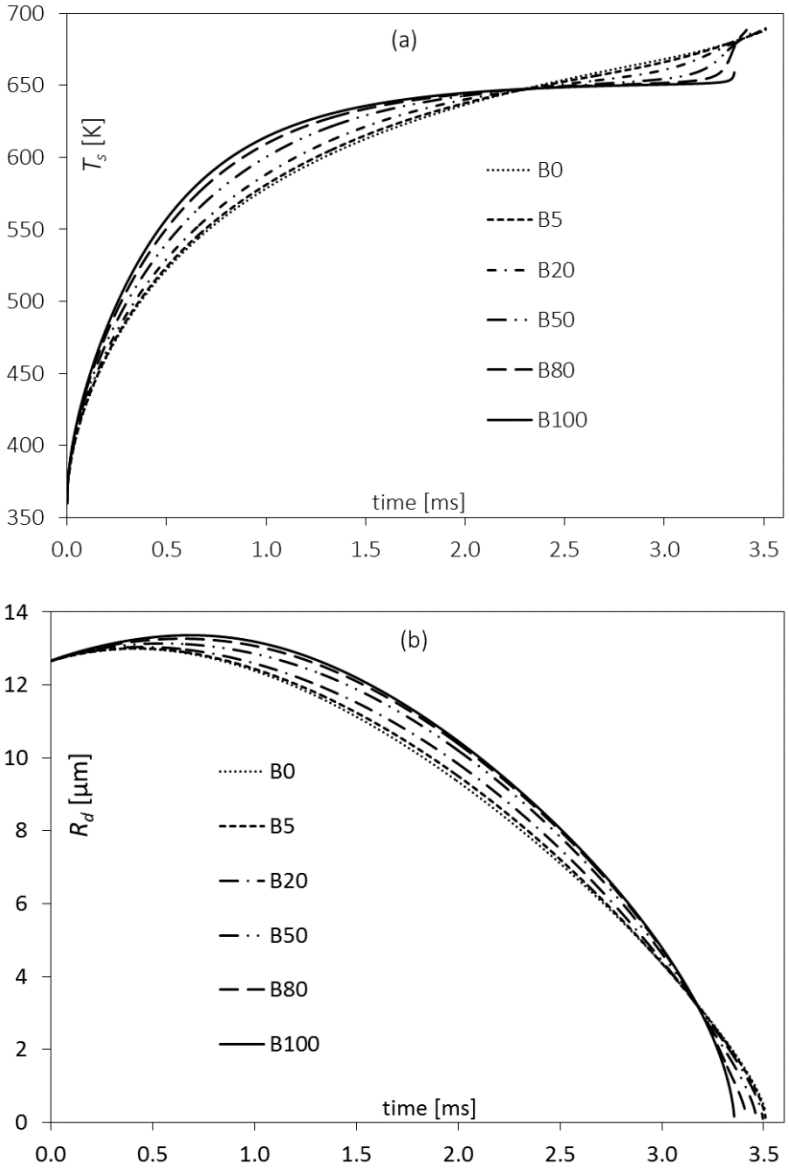

Fig. 1. The plots of droplet surface temperatures T_s (a), and radii R_d (b) versus time for various Diesel/SME blends, using the DC model.

As one can see from Fig. 1, the evaporation time of a pure SME (B100) droplet is 6% less than that of a pure Diesel (B0) droplet. Thus, the evaporation characteristics of Diesel and SME droplets are rather close. The predicted droplet surface temperature for B100 is higher than that of B0 during the initial heating period. This might enhance the droplet break-up process due to decrease in droplet surface tension [33].

The temporal evolutions of the liquid mass fractions at the droplet surface for representative components of B50 are shown in Fig. 2.

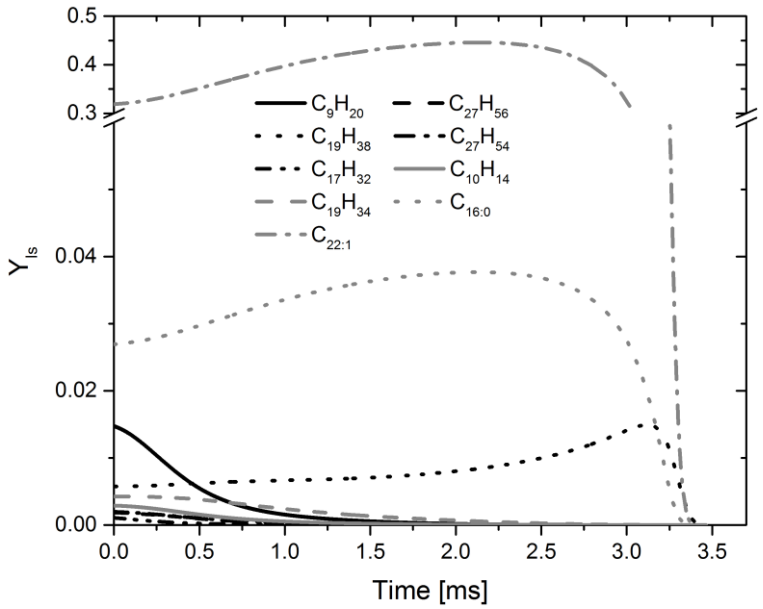

Fig. 2. The plots of surface liquid mass fractions Y_s of representative components versus time for a B50 fuel droplet for the same conditions as in Fig. 1.

As follows from Fig. 2, the mass fractions of the light components monotonically decrease with time while those of the heavy components monotonically increase with time. The mass fractions of the intermediate components initially increase but then decrease with time. One can expect this complex behaviour of different components to affect the distributions of mass fractions of components inside the combustion chamber in realistic engine conditions, where the ambient gas temperatures are not homogeneous.

It is not currently feasible to consider large numbers of components in CFD simulations. As shown in our previous papers [23,24], the application of the MDQD model would allow us to reduce the CPU requirements substantially without significant reduction in accuracy. In [23,24] this approach was applied to pure Diesel and pure gasoline fuel droplets. In what follows it is applied to blended biodiesel/Diesel fuel droplets.

The evolutions of droplet surface temperatures T_s and radii R_d over time for B50, predicted by the MDQD model for several C/QCs, are shown in Fig. 3. The following numbers of C/QCs were used: 105; 90, 63, 45, 25, 21, 19, 17, 12, and 10. The Diesel and biodiesel fuel components used in our analysis are shown in Tables 1 and 2 (see Appendix A for further details).

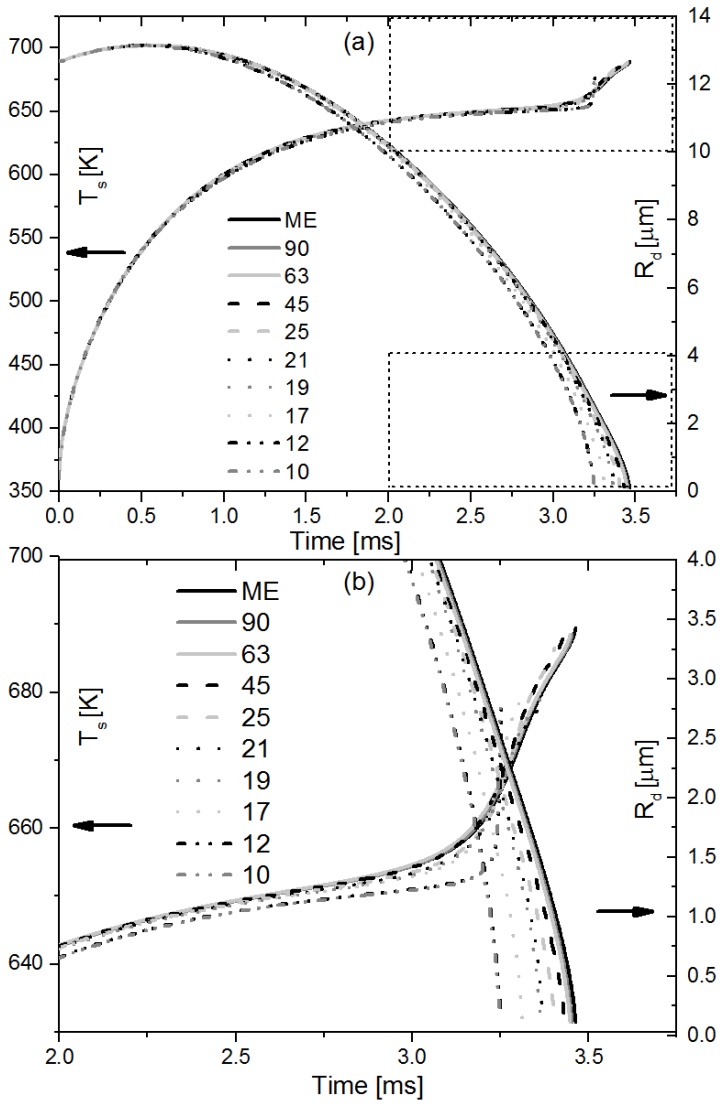

Fig. 3. The plots of the droplet surface temperatures T_s and radii R_d versus time for 10 approximations of B50: 105 components (ME); 90, 63, 45, 25, 21, 19, 17, 12, and 10 C/QCs (numbers near the curves); (b) Zoomed parts of (a). The compositions of these approximations are shown in Tables 1 and 2.

As follows from Fig. 3, the approximations of the blended fuel with 90, 63, 45, and 25 C/QCs lead to underestimation of the droplet lifetime by less than 3%. This underestimation increases to 4-6% for 20, 17 and 15 QCs. It further increases to 9%, 16% and 17% for 14, 9 and 7 QCs, respectively. The errors in predicted droplet surface temperatures for these C/QCs are negligible.

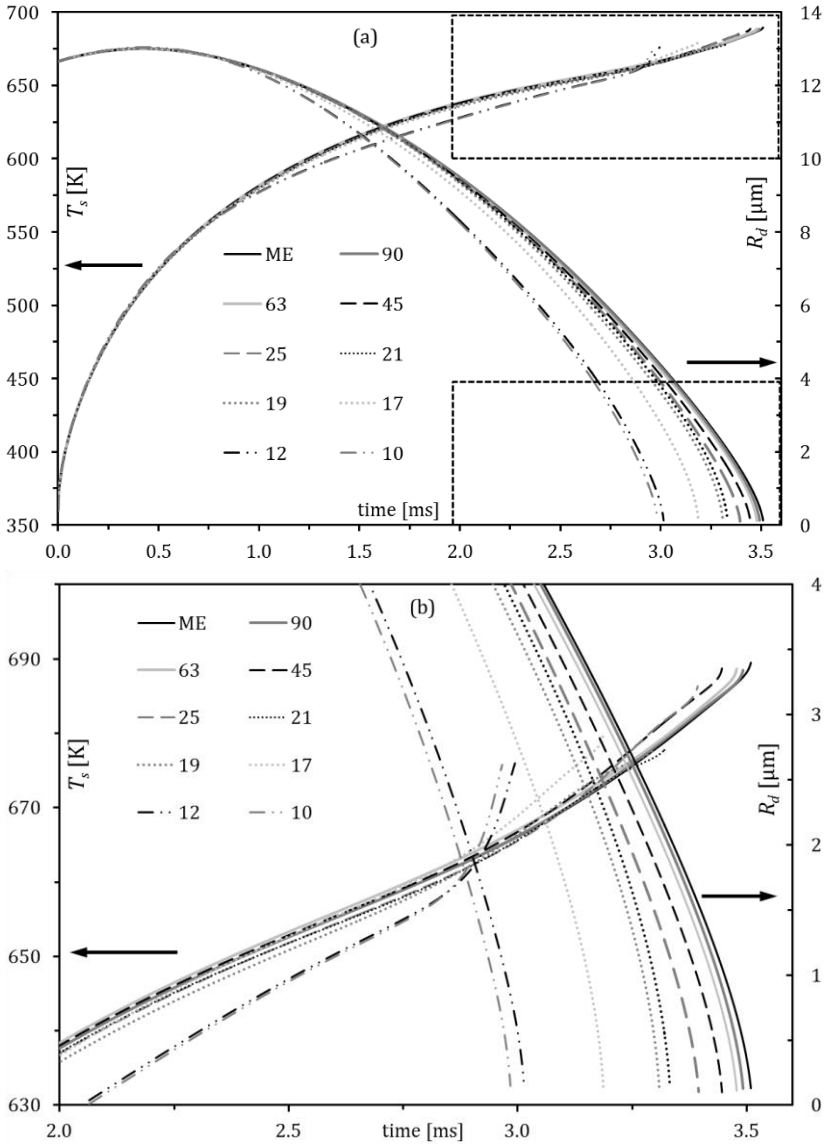

Fig. 4. The plots of the droplet surface temperatures T_s and radii R_d versus time for the same 10 approximations of B5 fuel as those used in Fig. 3; (b) Zoomed parts of (a). The compositions of these approximations are shown in Tables 1 and 2.

The evolutions of T_s and R_d over time for a B5 fuel droplet are shown in Fig. 4. Similarly to Fig. 3, in Fig. 4, the approximations of the blended fuel with up to 25 C/QCs lead to underestimation of the droplet lifetime by less than 3.2%. This underestimation increases to 5% for 21 and 19 C/QCs. It further increases to 9% for 17 C/QCs, and up to 15% for 12 and 10 C/QCs. The errors in predicted droplet surface temperatures for these approximations were up to 2%.

Swelling of the droplets can be clearly seen for all approximations of Diesel fuel due to changes in fuel density with temperature. Droplet surface temperature does not show plateau profiles. This can be attributed to the multi-component composition of droplets (see [23] for the details).

Note that the approximation of B50 fuel components with 17 C/QCs (Fig. 3) yields better results than using the same approximation for B5 fuel (Fig. 4). In the 17 C/QC approach, 4 C/QC of SME fuel out of 17 C/QC are taken into account. This approximation leads to a good balance between components for the case of B50 fuel. However, an increase in heavy C/QCs of SME at the expense of other components for B5 fuel near the end of evaporation time leads to over-estimation of the contribution of SME to B5.

Table 1. The contributions of Diesel and biodiesel fuel components for several choices of C/QCs shown in Figs. 3-4. The contributions of Diesel fuel components are specified in Table 2.

total C/QCs	Diesel C/QC	biodiesel C/QC	biodiesel C/QC						
105	98	7	C14:0	C16:0	C18:0	C20:0	C18:1	C18:2	C18:3
90	85	5	$C_{17.53}$ (C14:0-C18:0)			C20:0	C18:1	C18:2	C18:3
63	63	5				as above			
45	40	5				as above			
25	21	4	$C_{17.613}$ (C14:0- C20:0)				C18:1	C18:2	C18:3
21	17	4				as above			
19	15	4				as above			
17	14	3	$C_{17.613}$ (C14:0- C20:0)				C18:1	C18:2	ignored
12	9	3				as above			
10	7	3				as above			

Table 2. The contributions of Diesel fuel C/QCs for the numbers of C/QCs shown in Figs. 3-4 and Table 1.

total C/QCs	Diesel components	Diesel C/QCs (see Tables A1-A6 in Appendix A for further details)						
		alkanes	cycloakanes	bicycloalkanes	alkylbenzenes	indanes/ tetralines	naphthalenes	tricycloalkane, diaromatic, phenanthrene
105	98	20	18	16	17	13	11	3
90	85	19	17	8	16	12	10	3
63	58	19	9	8	8	6	5	3
45	40	10	9	5	8	3	2	3
25	21	5	4	3	3	3	2	tricycloalkane
21	17	4	3	2	3	2	2	tricycloalkane
19	15	4	3	1	3	2	1	tricycloalkane
17	14	4	2	1	2	1	1	3
12	9	1	1	1	1	1	1	3
10	7	1	1	1	1	1	1	tricycloalkane

To illustrate the computational efficiencies of these approximations, using the MDQD model, a diagram for CPU time required for these calculations versus the numbers of QC/Cs is shown in Fig. 5.

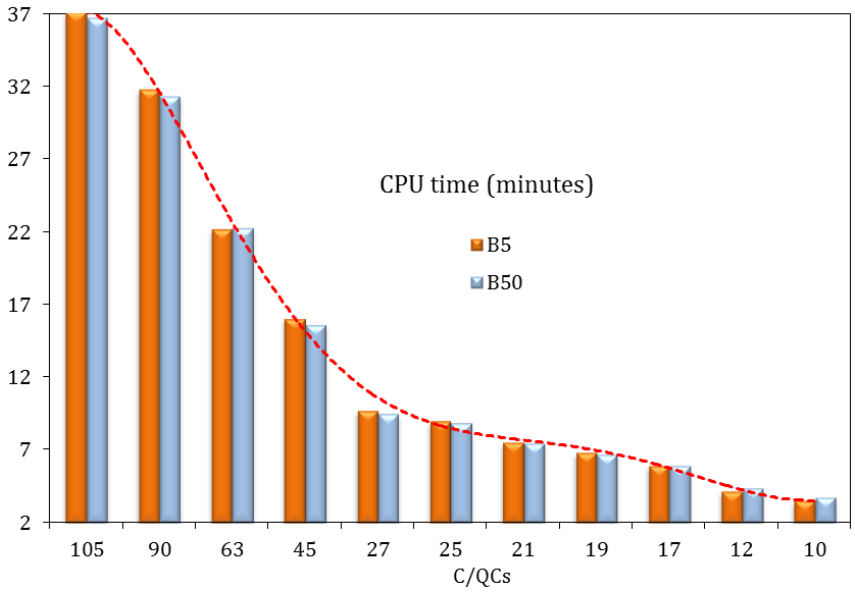

Fig. 5. The plot of CPU time required for calculations of droplet heating and evaporation versus the number of C/QCs for B5 and B50 fuel droplets, using the same parameters as in Figs. 1–4.

As can be seen from Fig. 5, approximating 105 components of the blended fuel with 17 C/QCs reduces the required CPU time by more than 83% compared with the model taking into account the contributions of all 105 components. Also, the results in Figs. 3 and 4 show that the evaporation time predicted for a 17 C/QC droplet is about 4% for B50, and 9% for B5, less than that predicted by the model taking into account the contributions of all 105 components. The predicted error in droplet surface temperatures when using 17 C/QCs is about 1%, for both B5 and B50 fuel droplets. Thus, the choice of 17 C/QCs can ensure a good compromise between CPU efficiency of the model and its accuracy when up to 9% and 4% errors in predicted droplet evaporation times can be tolerated for B5 and B50, respectively.

The specifications of the workstation used were: Z210, Intel core, 64-bit, 3.10 GHz and 8 GB RAM. The number of terms in the series in analytical solutions for temperature and species (see Equations (10), (11) and (19) in [23]) were taken equal to 44 and 33, respectively. The time step was set as 1 μs.

4. Conclusions

A new approach to modelling the heating and evaporation of blended biodiesel (soybean methyl ester, SME)/Diesel fuel droplets in representative conditions for a direct injection internal combustion engine is described. The full composition of fuel-blends with Diesel and SME contains up to 105 components. As in the

previously suggested multi-dimensional quasi-discrete (MDQD) model, these 105 components are replaced with a smaller number of components and quasi-components (C/QCs). Transient diffusion of these C/QCs in the liquid phase, temperature gradient, and recirculation inside droplets due to relative velocities between droplets and ambient air are taken into account based on the Effective Thermal Conductivity/Effective Diffusivity model.

It is shown that the approximation of the full composition of the blended fuel (105 components) by 17 C/QCs of B50 (50% SME and 50% Diesel) using the MDQD model leads to deviations in estimated droplet surface temperatures and evaporation times of up to 1% and 4%, respectively, which can be tolerated in many practical engineering applications. However, the choice of 17 C/QCs of B5 (5% SME and 95% Diesel) can lead to 9% error in predicted droplet evaporation time.

It is shown that the application of the MDQD model to B50 with 17 C/QCs leads to over 83% reduction in CPU time compared to the model which takes into account the contributions of all 105 components. The choice of 19 C/QCs of B5 leads to 82% reduction in CPU time. The error in estimated droplet lifetime in this case is shown to be about 5%.

Acknowledgement

One of the authors (S.S. Sazhin) is grateful to EPSRC (grants EP/K005758/1 and EP/M002608/1) for their financial support.

References

[1] Lapuerta M, Armas O, Rodriguezfernandez J. Effect of biodiesel fuels on diesel engine emissions. Prog Energy Combust Sci 2008;34:198–223. doi:10.1016/j.pecs.2007.07.001.

[2] Lapuerta M, Rodríguez-Fernández J, Armas O. Correlation for the estimation of the density of fatty acid esters fuels and its implications. A proposed Biodiesel Cetane Index. Chem Phys Lipids 2010;163:720–7. doi:10.1016/j.chemphyslip.2010.06.004.

[3] Meher LC, Vidya Sagar D, Naik SN. Technical aspects of biodiesel production by transesterification—a review. Renew Sustain Energy Rev 2006;10:248–68. doi:10.1016/j.rser.2004.09.002.

[4] Dunn RO. Cold-Flow Properties of Soybean Oil Fatty Acid Monoalkyl Ester Admixtures. Energy Fuels 2009;23:4082–91. doi:10.1021/ef9002582.

[5] Hill J, Nelson E, Tilman D, Polasky S, Tiffany D. Environmental, economic, and energetic costs and benefits of biodiesel and ethanol biofuels. Proc Natl Acad Sci 2006;103:11206–10. doi:10.1073/pnas.0604600103.

[6] Pan K-L, Li J-W, Chen C-P, Wang C-H. On droplet combustion of biodiesel fuel mixed with diesel/alkanes in microgravity condition. Combust Flame 2009;156:1926–36. doi:10.1016/j.combustflame.2009.07.020.

[7] Tickell J, Roman K. From the Fryer to the Fuel Tank: the Complete Guide to Using Vegetable Oil as an Alternative Fuel. New Orleans, LA: Joshua Tickell Media Productions; 2003.

[8] US Department of Energy: Energy Efficiency and Renewable Energy. Biodiesel Blends n.d. http://www.afdc.energy.gov/fuels/biodiesel_blends.html (accessed October 13, 2015).

[9] EPA U. US Environmental Protection Agency 2014. http://www.epa.gov/ (accessed November 15, 2014).

[10] Yuan W, Hansen AC, Zhang Q. Predicting the physical properties of biodiesel for combustion modeling. Trans ASAE 2003;46:1487–93. doi:10.13031/2013.15631.

[11] Sazhin SS. Droplets and Sprays. London: Springer; 2014.

[12] Al Qubeissi M. Heating and Evaporation of Multi-Component Fuel Droplets. Stuttgart: WiSa; 2015.

[13] Samimi Abianeh O, Chen CP. A discrete multicomponent fuel evaporation model with liquid turbulence effects. Int J Heat Mass Transf 2012;55:6897–907. doi:10.1016/j.ijheatmasstransfer.2012.07.003.

[14] Ra Y, Reitz RD. A vaporization model for discrete multi-component fuel sprays. Int J Multiph Flow 2009;35:101–17. doi:10.1016/j.ijmultiphaseflow.2008.10.006.

[15] Zhu G-S, Reitz RD. A model for high-pressure vaporization of droplets of complex liquid mixtures using continuous thermodynamics. Int J Heat Mass Transf 2002;45:495–507. doi:10.1016/S0017-9310(01)00173-9.

[16] Laurent C, Lavergne G, Villedieu P. Continuous thermodynamics for droplet vaporization: Comparison between Gamma-PDF model and QMoM. Comptes Rendus Mécanique 2009;337:449–57. doi:10.1016/j.crme.2009.06.004.

[17] Grote M, Lucka K, Köhne H. Multicomponent droplet evaporation of heating oil using a continuous thermodynamics model. V ECCOMAS CFD, Lisbon, Portugal: 2010.

[18] Burger M, Schmehl R, Prommersberger K, Schäfer O, Koch R, Wittig S. Droplet evaporation modeling by the distillation curve model: accounting for kerosene fuel and elevated pressures. Int J Heat Mass Transf 2003;46:4403–12. doi:10.1016/S0017-9310(03)00286-2.

[19] Smith BL, Bruno TJ. Advanced Distillation Curve Measurement with a Model Predictive Temperature Controller. Int J Thermophys 2006;27:1419–34. doi:10.1007/s10765-006-0113-7.

[20] Qi DH, Lee CF. Influence of soybean biodiesel content on basic properties of biodiesel-diesel blends. J Taiwan Inst Chem Eng 2014;45:504–7. doi:10.1016/j.jtice.2013.06.021.

[21] Sazhin SS, Elwardany A, Krutitskii PA, Castanet G, Lemoine F, Sazhina EM, et al. A simplified model for bi-component droplet heating and evaporation. Int J Heat Mass Transf 2010;53:4495–505. doi:10.1016/j.ijheatmasstransfer.2010.06.044.

[22] Elwardany AE, Gusev IG, Castanet G, Lemoine F, Sazhin SS. Mono- and multi-component droplet cooling/heating and evaporation: comparative analysis of numerical models. **Atom Sprays** 2011;21:907–31. doi:10.1615/AtomizSpr.2012004194.

[23] Sazhin SS, Al Qubeissi M, Nasiri R, Gun'ko VM, Elwardany AE, Lemoine F, et al. A multi-dimensional quasi-discrete model for the analysis of Diesel fuel droplet heating and evaporation. Fuel 2014;129:238–66. doi:10.1016/j.fuel.2014.03.028.

[24] Al Qubeissi M, Sazhin SS, Turner J, Begg S, Crua C, Heikal MR. Modelling of gasoline fuel droplets heating and evaporation. Fuel 2015;159:373–84. doi:10.1016/j.fuel.2015.06.028.

[25] Elwardany AE, Sazhin SS. A quasi-discrete model for droplet heating and evaporation: Application to Diesel and gasoline fuels. Fuel 2012;97:685–94. doi:10.1016/j.fuel.2012.01.068.

[26] Abramzon B, Sazhin SS. Convective vaporization of a fuel droplet with thermal radiation absorption. Fuel 2006;85:32–46. doi:10.1016/j.fuel.2005.02.027.

[27] Sazhin SS, Al Qubeissi M, Kolodnytska R, Elwardany AE, Nasiri R, Heikal MR. Modelling of biodiesel fuel droplet heating and evaporation. Fuel 2014;115:559–72. doi:10.1016/j.fuel.2013.07.031.

[28] Dooley S, Uddi M, Won SH, Dryer FL, Ju Y. Methyl butanoate inhibition of n-heptane diffusion flames through an evaluation of transport and chemical kinetics. Combust Flame 2012;159:1371–84. doi:10.1016/j.combustflame.2011.09.016.

[29] Al Qubeissi M, Sazhin SS, Crua C, Turner J, Heikal MR. Modelling of biodiesel fuel droplet heating and evaporation: effects of fuel composition. Fuel 2015;154:308–18. doi:10.1016/j.fuel.2015.03.051.

[30] Sazhin SS, Krutitskii PA, Abdelghaffar WA, Sazhina EM, Mikhalovsky SV, Meikle ST, et al. Transient heating of diesel fuel droplets. Int J Heat Mass Transf 2004;47:3327–40. doi:10.1016/j.ijheatmasstransfer.2004.01.011.

[31] Ali OM, Mamat R, Abdullah NR, Abdullah AA. Analysis of blended fuel properties and engine performance with palm biodiesel–diesel blended fuel. Renew Energy 2016;86:59–67. doi:10.1016/j.renene.2015.07.103.

[32] Candeia RA, Silva MCD, Carvalho Filho JR, Brasilino MGA, Bicudo TC, Santos IMG, et al. Influence of soybean biodiesel content on basic properties of biodiesel–diesel blends. Fuel 2009;88:738–43. doi:10.1016/j.fuel.2008.10.015.

[33] Bormashenko E. Surface instabilities and patterning at liquid/vapor interfaces: Exemplifications of the "hairy ball theorem". Colloids Interface Sci Commun 2015;5:5–7. doi:10.1016/j.colcom.2015.04.003.

Appendix A. C/QCs approximating Diesel fuel compositions

The detailed compositions of the groups of C/QCs shown in Table 2 are presented in the following tables.

Table A1. The numbers of C/QCs (top numbers), and the corresponding compositions of C/QCs, described in terms of carbon atoms (columns of numbers), used in the MDQD model for alkanes.

alkanes (C_nH_{2n+2})					
20	19	10	5	4	1
8	8	8.91 (C8-C9)	9.958 (C8-11)	10.335 (C8-C12)	14.763 (C8-C27)
9	9				
10	10	10.385 (C10-11)			
11	11				
12	12	12.493 (C12-13)	13.58 (C12-C15)		
13	13				
14	14	14.544 (C14-C15)		15.046 (C13-C17)	
15	15				
16	16	16.518 (C16-C17)			
17	17		17.622 (C16-C19)		
18	18	18.521 (C18-19)			
19	19				
20	20	20.392 (C20-C21)		19.38 (C18-C22)	
21	21		20.869 (C20-C23)		
22	22	22.332 (C22-C23)			
23	23				
24	24	24.344 (C24-C25)	24.763 (C24-C27)	23.842 (C23-C27)	
25	25				
26	26.421 (C26-C27)	26.421 (C26-C27)			
27					

Table A2. The numbers of C/QCs (top numbers), and the corresponding compositions of C/QCs, described in terms of carbon atoms (columns of numbers), used in the MDQD model for cycloalkanes.

cycloalkanes (C_nH_{2n})						
18	17	9	4	3	2	1
10	10	10.745 (C10-C11)				
11	11		12.122 (C10-14)			
12	12	12.427 (C12-C13)		12.562 (C10-C15)		
13	13				13.88 (C10-C18)	
14	14	14.475 (C14-C15)				
15	15					
16	16	16.493 (C16-C17)	17.081 (C15-C19)			
17	17					15.365 (C10-C27)
18	18	18.513 (C18-C19)		18.297 (C16-C21)		
19	19					
20	20	20.35 (C20-C21)				
21	21		20.878 (C20-C24)		20.254 (C19-C27)	
22	22	22.264 (C22-C23)		22.977 (C22-C27)		
23	23					
24	24	24.37 (C24-C25)				
25	25		25.644			

26	26.42	26.42	(C25-C27)
27	(C26-C27)	(C6-C27)	

Table A3. The numbers of C/QCs (top numbers), and the corresponding compositions of C/QCs, described in terms of carbon atoms (columns of numbers), used in the MDQD model for bicycloalkanes.

bicycloalkanes (C_nH_{2n-2})					
16	8	5	3	2	1
10	10.603	11.104	11.835	13.065	14.743
11	(C10-C11)	(C10-C12)	(C10-C14)	(C10-C17)	(C10-C25)
12	12.404				
13	(C12-C13)	13.861			
14	14.434	(C13-C15)			
15	(C14-C15)				
16	16.57	17.091	17.397		
17	(C16-C17)	(C16-C18)	(C15-C19)		
18	18.602				
19	(C18-C19)	19.3			
20	20.322	(C19-C21)		19.168	
21	(C20-C21)			(C18-C25)	
22	22.41		21.243		
23	(C22-C23)	22.919	(C20-C25)		
24	24.419	(C22-C25)			
25	(C24-C25)				

Table A4. The numbers of C/QCs (top numbers), and the corresponding compositions of C/QCs, described in terms of carbon atoms (columns of numbers), used in the MDQD model for alkylbenzenes.

alkylbenzenes (C_nH_{2n-6})					
17	16	8	3	2	1
8	8	8.867			
9	9	(C8-C9)			
10	10	10.15	10.207		
11	11	(C10-C11)	(C8-C13)		
12	12	12.264		10.726	
13	13	(C12-C13)		(C8-C16)	
14	14	14.425			
15	15	(C14-C15)			11.726
16	16	16.475	16.233		(C8-C24)
17	17	(C16-C17)	(C14-C19)		
18	18	18.381			
19	19	(C18-C19)			
20	20	20.416		19.026	
21	21	(C20-C21)		(C17-C24)	
22	22		21.077		
23	23.489	22.743	(C20-C24)		
24	(C23-C24)	(C22-C24)			

Table A5. The numbers of C/QCs (top numbers), and the corresponding compositions of C/QCs, described in terms of carbon atoms (columns of numbers), used in the MDQD model for indanes/tetralines.

indanes/tetralines (C_nH_{2n-8})					
13	12	6	3	2	1
10	10	10.509 (C10-C11)	11.407 (C10-C13)	12.495 (C10-16)	13.832 (C10-C22)
11	11				
12	12	12.471 (C12-C13)			
13	13				
14	14	14.456 (C14-C15)	15.342 (C14-C17)		
15	15				
16	16	16.456 (C16-C17)			
17	17				
18	18	18.388 (C18-C19)	19.242 (C18-C22)	18.615 (C17-C22)	
19	19				
20	20	20.567 (C20-C22)			
21	21.32 (C21-C22)				
22					

Table A6. The numbers of C/QCs (top numbers), and the corresponding compositions of C/QCs, described in terms of carbon atoms (columns of numbers), used in the MDQD model for naphthalenes.

naphthalenes (C_nH_{2n-12})				
11	10	5	2	1
10	10	10.566 (C10-C11)	11.533 (C10-C15)	12.392 (C10-C20)
11	11			
12	12	12.354 (C12-C13)		
13	13			
14	14	14.441 (C14-C15)		
15	15			
16	16	16.421 (C16-C17)	17.904 (C16-C20)	
17	17			
18	18	18.985 (C18-C20)		
19	19.51 (C19-C20)			
20				